# $T_c$ degradation in cuprate superconductors from the resistivity of $YBa_2(Cu_{1-x}M_x)_4O_8$ for $M$ = Fe and Ni

Ratan Lal, V. P. S. Awana, S. P. Pandey, V. S. Yadav, Deepak Varandani, and A. V. Narlikar
*National Physical Laboratory, K.S. Krishnan Road, New Delhi 110012, India*

Anjli Chhikara
*Department of Physics, Goa University, Goa, India*

E. Gmelin
*Max-Planck-Institut für Festkörperforschung, Heisenbergstrasse 1, D-70569, Stuttgart, Germany*
(Received 6 January 1994; revised manuscript received 12 August 1994)

Systematic measurements of the resistivity of the polycrystalline samples of the $YBa_2(Cu_{1-x}M_x)_4O_8$ system with $M$=Fe, Ni are reported. The resistivity behavior depends strongly on the dopant concentration. For the Fe 6-at. % sample, there is no metallic behavior in the resistivity, but for $T > 50$ K, the resistivity decreases very slowly with temperature. The behavior of the resistivity of the Fe 10-at. % and Ni 5-at. % samples is analyzed, and it is found that the variable-range hopping process may occur in these samples below about 30 K. While the Ni 5-at. % sample is found to show signs of the nearest-neighbor hopping process of conductivity above about 150 K, the Fe 10-at. % sample does not show such behavior up to 300 K. On this basis it is found that localization may not be a possible reason of the large $T_c$ depression in the $YBa_2(Cu_{1-x}M_x)_4O_8$ system by the Fe and Ni dopants. We have examined the possibility of $T_c$ degradation due to carrier-impurity potential scattering also by using a single-crystal analog of the polycrystalline sample. This analogy is justified to within a factor of less than 1.33. On the basis of this analogy we have found that potential scattering may not be a reasonable source of $T_c$ degradation in the Ni- and Fe-doped samples of the system considered.

## I. INTRODUCTION

The problem of $T_c$ degradation by $3d$ metallic (and other) impurities in the cuprate superconductors is as complex as the problem of occurrence of superconductivity in the clean phase of these systems. Experimentally it has been found that $3d$ metallic impurities (Fe, Co, Ni, Zn, and Ga) suppresses $T_c$ in the cuprate systems much more strongly than in the conventional superconductors.[1,2] There are principally four known reasons of $T_c$ degradation in the impurity-doped superconductors. They are localization,[3] magnetic pair breaking[4] (for $s$-wave pairing), potential scattering (for $d$-wave pairing),[5] and direct suppression of the effective pairing interaction.[2,6] In the case of cuprate superconductors Walstedt *et al.*[7] have found very recently that the magnetic pair breaking is inadequate in the Zn-doped $YBa_2Cu_3O_7$ (Y123) system. A similar conclusion is drawn by Lal *et al.*[2] on the basis of the $T_c$ degradation in the dirty $YBa_2Cu_4O_8$ (Y124) and Y123 systems. If the nature of pairing in cuprate superconductors is of $d$-wave type, then $T_c$ degradation may be due to potential scattering from the impurity.[5,7] But whether cuprate superconductors have $d$-wave pairing or $s$-wave pairing is not clear at present because there are evidences in favor of both of them.[8,9] Thus a mechanism of $T_c$ degradation based on potential scattering may be reasonable in cuprates. Whether $T_c$ degradation in cuprates is due to localization or potential scattering can be ascertained to some extent by the measured resistivity of cuprate systems doped with different $3d$ metallic impurities. However, since the carriers are limited mostly to the $ab$ plane, and since the cuprate superconductors are highly anisotropic,[10,11] we should consider single crystals or epitaxial thin films for the resistivity measurements. But we have not yet succeeded in preparing single-crystal samples of Y124 doped with different $3d$ metallic impurities. In fact, there are many difficulties in the way of preparing a single crystal or epitaxial film of Y124 doped with $3d$ metallic impurities. The main trouble arises due to the presence of Y123.

For the study of localization effects we expect no problem due to the polycrystalline nature of the samples, because the scaling theory of localization[12] does not permit anisotropic localization (even) in an anisotropic system. As far as the carrier-impurity potential scattering is concerned, we need the scattering rate for the process corresponding to the $ab$ plane. In the absence of single crystals of the doped Y124 systems, it is advantageous to represent the polycrystalline samples of Y124 by their "single-crystal-analog" samples of $ab$ plane resistivity[13]

$$\tilde{\rho}_{ab} = [\gamma(x)]^{-2/3}\rho(x) \ . \tag{1}$$

Here $\gamma(x) = (\rho_c/\rho_{ab})^{1/2}$, with $\rho_c$ as the $c$-direction resistivity and $\rho_{ab}$ as the $ab$-plane resistivity, is used to characterize the anisotropy ratio[10,11] of the sample. (According to Ref. 10, $\gamma_{124} \approx 2\gamma_{123}$.) In the Appendix we have found that from the view-point of resistivity the

 

analogy of the single-crystal analog of the polycrystalline samples is justified to within a factor of about 1.33. In the absence of resistivity data of actual single-crystal samples, one may therefore employ the polycrystalline samples to study the localization and carrier-impurity potential scattering effects. The result of this type of study will be uncertain by a factor of about 1.33. We have measured the resistivity of the superconducting and nonsuperconducting Fe- and Ni-doped Y124 systems for those impurity concentrations for which the corresponding Y123 system is superconducting. The localization effect is obtained from the resistivity data of Fe- and Ni-doped nonsuperconducting Y124 samples, while the carrier-impurity potential scattering rate has been obtained from the resistivity data of the superconducting samples.

## II. EXPERIMENTAL

Samples with nominal compositions $YBa_2(Cu_{1-x}M_x)_4O_8$ ($M$ = Fe and Ni) have been prepared at ambient pressure of oxygen using $Na_2C_2O_4$ as catalyst[14] by solid-state reaction of stoichiometric mixtures of the constituent oxides. $Y_2O_3$, $Ba(NO_3)_2$, CuO, $Fe_2O_3$, and NiO, each of 99.99% purity, were used as starting ingredients. These were mixed in the stoichiometric ratio required for each sample along with 0.2 mole fraction of sodium oxalate. The synthesis process is relatively simple, involving two steps. In the first step, the homogeneously mixed constituents were prereacted in the powder form for 30 min at 900 °C and then cold pressed into rectangular bars which were again reacted for 24 h at 900 °C in a continuous flow of oxygen. In the second step the reaction temperature was reduced to 815 °C for another 48 h.

Measurements of the temperature dependence of resistivity were carried out using the standard four-probe technique. Air-drying silver paste was used to make electrical contacts on the samples. The temperature of the sample was monitored using a Ge sensor. The measurement system was hooked to a HP-216 system controller for automatic data acquisition and processing. The x-ray diffraction pattern of the samples were recorded using a Siemens D-500 x-ray diffractometer with Cu $K\alpha$ radiation. The ac susceptibility of a pure Y124 sample was measured using Lakeshore ac susceptometer model 7000.

## III. RESULTS

Powder x-ray diffraction patterns of Y124 sample, substituted with 1, 4, 6, and 10 at. % Fe were taken at room temperature. For the Fe 1-at. % and 4-at. % samples, all the diffraction peaks were indexed by the orthorhombic structure of the 1-2-4 phase. Orthorhombicity of these samples was clearly visible through the splitting of [017],[111] and [020],[200] planes. In the 6-at. % and 10-at. % Fe-substituted samples, a transition from orthorhombic to tetragonal behavior was quite evident from the overlapping of [020],[200] and [017],[111] planes. The x-ray diffraction data confirm the previous report[15,16] that the $YBa_2Cu_4O_8$ structure suffers from structural variations with gradual increase of Fe content in the 1-2-4 lattice. The parameters of the Fe-doped system are shown in Fig. 1.

Powder x-ray diffraction (XRD) patterns of and pure Y124 samples substituted with 1, 3, and 5 at. % Ni were also obtained at room temperature. In all the samples (pure and Ni substituted) most of the diffraction peaks were indexed by the orthorhombic structure of the 1-2-4 phase. These x-ray data confirmed the previous report[17,18] that the Y124 structure is less affected by Ni substitution. The XRD pattern of the Ni-substituted Y124 samples also indicated that in all the samples of $YBa_2(Cu_{1-x}Ni_x)_4O_8$ with $x = 0.01-0.05$ the crystal structure remains invariant. The orthorhombicity of the system does not seem to be affected by Ni substitution, as evidenced through the unaffected splittings of the [017],[111] and [020],[200] planes. The lattice parameter values (Fig. 2) do not change significantly with increase of Ni content in the samples.

The temperature dependence of the ac susceptibility of the pure Y124 sample is shown in Fig. 3. The measurements were performed in a field of 0.1 Oe rms by increasing the temperature from 63 K upwards. The diamagnetic onset starts around 75 K. The $\chi'$ curve is sharp and saturation is observed around 62 K. Also, there is a peak in the $\chi''$ curve around 68 K, corresponding to the sharp drop in $\chi'$, which is an indication of intergranular coupling. The $T_c$ degradation in Fe- and Ni-doped Y124, as reported in Ref. 2, is confirmed by resistivity measurements of the Fe- and Ni-doped samples [Figs. 4(a) and 4(b)]. The resistivity versus temperature behavior of the superconducting as well as nonsuperconducting samples of Fe- and Ni-doped Y124 is presented in Figs. 4(a)–4(c) for $10 < T < 300$ K.

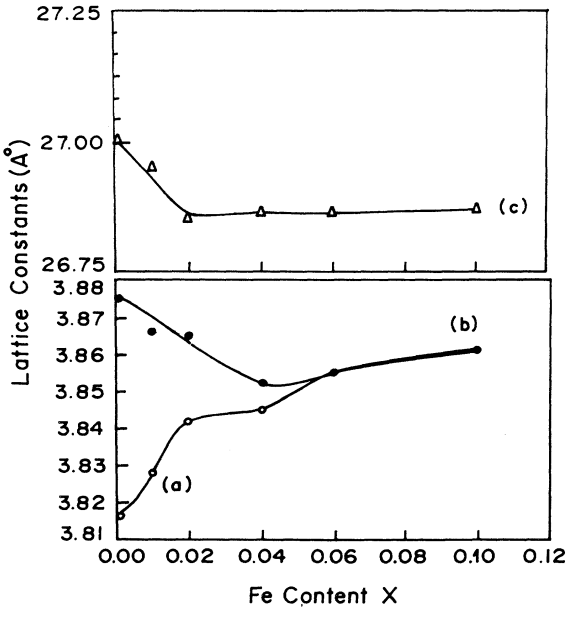


FIG. 1. Variation of the lattice parameters $a$, $b$, and $c$ with $x$ for the $YBa_2(Cu_{1-x}Fe_x)_4O_8$ samples.

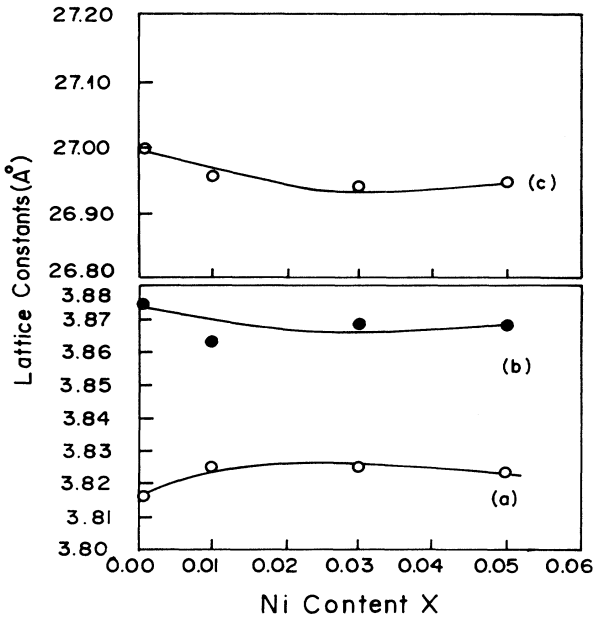


FIG. 2. Variation of the lattice parameters $a$, $b$, and $c$ with $x$ for the $YBa_2(Cu_{1-x}Ni_x)_4O_8$ samples.

## IV. DISCUSSION

### A. Localization and superconductivity

In order to extract information from the resistivity data on the effects of Fe and Ni dopants on the $T_c$ degradation, we first of all calculate the localization length[19] corresponding to the Fe 10-at. % and Ni 5-at. % samples of Y124. The localization length in the $x<0.1 (x<0.5)$ samples of Fe (Ni) will definitely be larger[20] than that of these samples. For this purpose we consider the process of electrical conductivity in the system considered. Possible mechanisms of electric conduction are (1) weak localization, (2) the Kondo effect, (3) variable-range hopping (VRH), and (4) nearest-neighbor hopping (NNH). We start from the VRH process. First of all, we identify the temperature range of the variable-range hopping process of conductivity in these samples. According to Mott's VRH law,[21] for constant density of states at the Fermi level, the resistivity $\rho$ behaves as $\ln(\rho/\rho_0) = (T_0/T)^{1/(1+d)}$ for the $d$-dimensional VRH process. Here the parameter $\rho_0$ depends on the material specifications; it can have a weak $T$ dependence also; $T_0 \approx \beta/k_B g t^{3-d}\xi^d$ is the temperature below which the localization process will take place. Here $t$ is the sample thickness, $k_B$ is the Boltzmann constant, $g$ is the density of states at the Fermi energy, and $\xi$ is the localization

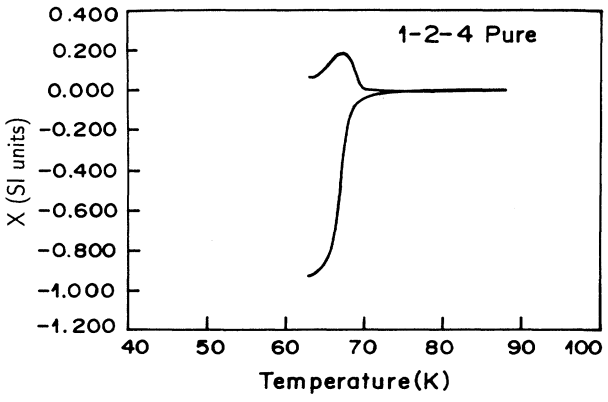


FIG. 3. ac susceptibility of pure $YBa_2Cu_4O_8$ specimen at 0.1 Oe rms.

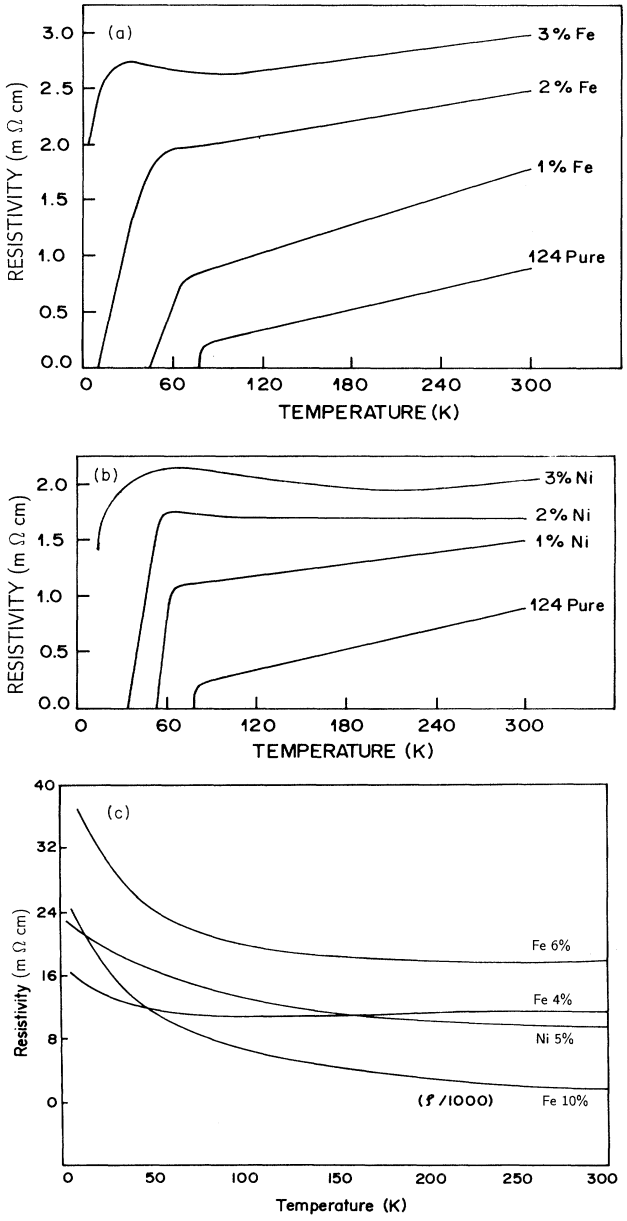


FIG. 4. $R$-$T$ plots for $YBa_2Cu_4O_8$ samples at different doping levels of Fe [(a) and (c)] and Ni [(b) and (c)].

length. The parameter $\beta \approx 21$ for $d=3$, and $\beta \approx 14$ for $d=2$.[21]

In Fig. 5 we have plotted $\ln\rho$ vs $T^{-1/3}$ and $T^{-1/4}$ to find the temperature range of the VRH regime. We find that for the Fe 10-at. % sample, two-dimensional (2D) or 3D VRH is not possible above ~20 K, while for the Ni 5-at. % sample 2D VRH is not possible above ~60 K, and 3D VRH is not possible above ~40 K. In any case, the temperature range from 10 K to these temperature values is so small that on the basis of Fig. 5 it is difficult to identify the extent and dimensionality of the VRH process. At most, the temperature range $T \sim 10$–$30$ K can be thought of as being the boundary region of the VRH regime from the low-$T$ side. For further clarification of the variable-range hopping regime and its dimensionality, we have made a plot of the logarithm of the localization energy $E_a = d(\ln\rho)/d(1/T)$ vs the logarithm of the inverse temperature $1/T$ in Fig. 6. It is seen that only the portion from $T=10$ K to $T \sim 30$ K, which is not more than an end region of the suspected low-$T$ VRH regime, corresponds to the VRH process. As shown in Fig. 6, the $T<30$ K points on the plot can be fitted with the slopes of $-\frac{2}{3}$ and $-\frac{3}{4}$ without a clear distinction. So the question of the VRH dimensionality cannot be answered with certainty on the basis of the small temperature range of 10–30 K. But it is not difficult to see that a slope of $-\frac{1}{2}$ will be a relatively poor fitting to the $T<30$ K points. So it may be said that the Abeles law of the VRH process,[22] namely, $\ln\rho \sim T^{-1/2}$, is unlikely to occur around or below 30 K. Taking the above results together means that in the Fe 10-at. % and Ni 5-at. % samples of Y124, the VRH process of conductivity can only take place at temperatures below about 30 K.

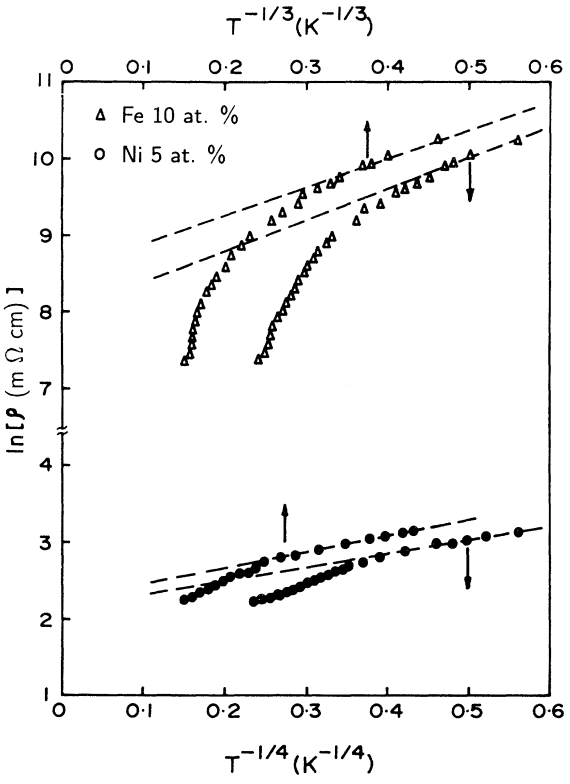


FIG. 5. Plot of $\ln\rho$ vs $T^{-1/3}$ and $\ln\rho$ vs $T^{-1/4}$ for the Fe 10-at. % and Ni 5-at. % samples. The value of $T_0$ is found to be 8.0, 11.6, 52.7, and 301.4 K, respectively, for the Ni 5-at. % (2D VRH), Ni 5-at. % (3D VRH), Fe 10-at. % (2D VRH), and Fe 10-at. % (3D VRH) samples.

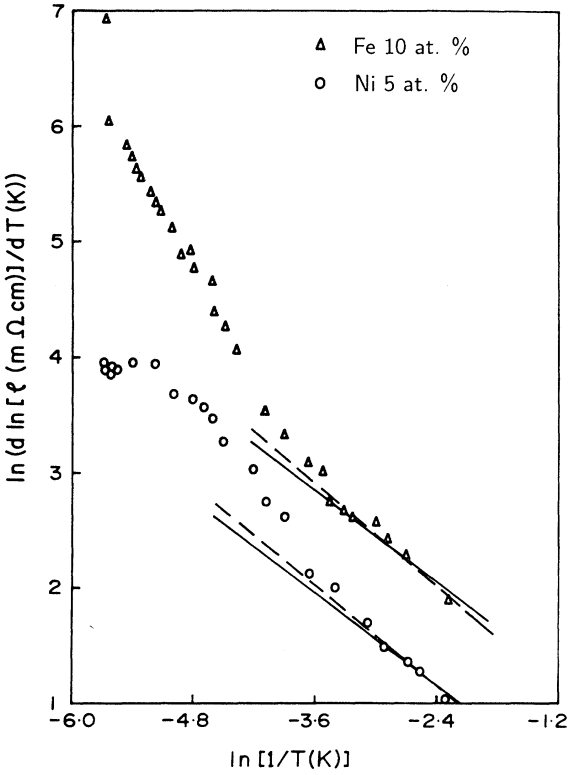


FIG. 6. Plot of the logarithm of the local activation energy $[d\ln(\rho)/d(1/T)]$ vs logarithm of the inverse temperature $1/T$ for the samples of Fig. 5. The solid lines correspond to the slope of $-\frac{2}{3}$ (2D VRH process), while the dashed lines correspond to the slope of $-\frac{3}{4}$ (3D VRH process). The plots do not show that either of these slopes is a better fit.

It is well known that with increasing temperature there takes place a transition from the VRH process of conductivity to the nearest-neighbor hopping process of conductivity.[23] However, there is yet no way to ascertain the width of the transition region.[23] Theoretically, the value of the local activation energy $E_a$ in the NNH regime should be three times greater than that at the transition point from the VRH side.[23] Furthermore, in the case of the full NNH process, the local activation energy $E_a$ should be independent of $T$. This is seen to occur in Fig. 6 only for the Ni 5-at. % sample above 150 K. One-third of this temperature is 50 K, which indicates the temperature below which the VRH process should occur in the Ni 5-at. % sample, we do not see any saturation of this sort of the local activation energy up to 300 K. This means that in the temperature range considered the Ni 5-at. % sample is expected to have a NNH process of

conductivity above 150 K, while the Fe 10-at. % sample will not. A $-\ln T$ contribution may be reasonable for the Fe 10-at. % sample. Physically such a contribution is expected from the Kondo effect[4] or weak localization,[5] and is associated with a change of density of states at the Fermi energy.

From the straight-line portions of the traces in Fig. 5, we find that $T_0 \sim 10$ K for the Ni 5-at. % sample, while $T_0 \sim 100$ K for the Fe 10-at. % sample. These values of $T_0$ correspond to $gt^{3-d}\xi^d \sim 10^4$ states per eV per localization volume for the Ni 5-at. % sample, and to $gt^{3-d}\xi^d \sim 10^3$ states per eV per localization volume for the Fe 10-at. % sample. This means that[24] $\xi \geq 100$ Å for the Ni 5-at. % sample, and $\xi \geq 40$ Å for the Fe 10-at. % sample. These values of $\xi$ are much larger than the coherence length of the clean system, $\xi_{\rm coh} \approx 5-20$ Å. This means that, according to the resistivity data of the Ni 5-at. % and Fe 10-at. % samples of Y124, the carrier localization in the samples considered is expected to be of less extent.

We now turn to the occurrence of superconductivity in the Fe- and Ni-doped Y124 system. For the $YBa_2(Cu_{1-x}Fe_x)_4O_8$ system, superconductivity is destroyed completely below $x = 0.04$ [Fig. 4(a)]. According to Ref. 19 $\xi$ increases rapidly with decrease of resistivity. Since we have also used the VRH process to obtain the value of $\xi$, we expect $\xi$ to increase rapidly for decreasing $x$. Thus in the $x < 0.03$ samples of Fe- and Ni-doped Y124 $\xi$ is expected to be larger than $\xi_{\rm coh}$. This means that in the $x < 0.03$ Fe- and Ni-doped samples the localization length may be much larger than the pure-sample coherence length $\xi_{\rm coh}$, and so the $x < 0.03$ disorder may not be sufficient to destroy superconductivity, because for that to happen we require $\xi \leq \xi_{\rm coh}$. We emphasize that this result will not change if we use data from a single crystal of Y124, because localization remains isotropic even for an anisotropic system.[12]

### B. Carrier-impurity potential scattering

For $d$-wave pairing the carrier self-energy due to the carrier-impurity potential scattering will be different in the normal and superconducting states. Because of this superconductivity will be suppressed; the rate of suppression will depend on the strength of the scattering rate. The carrier-impurity scattering rates for Fe- and Ni-doped Y124 can be obtained from the resistivity data of the superconducting samples by calculating the slope $d\rho_{\rm res}/dx$ for low $x$. Here $\rho_{\rm res}$ is the $T = 0$ value of the extrapolation of the linear part of the resistivity. According to Tarascon *et al.*,[25] the average value of $d\rho_{\rm res}/dx$ for Fe-doped Y123 of low $x$ is $\approx 45$ mΩ cm per Fe concentration, while for Ni-doped Y123 it is $\approx 1.8$ mΩ cm per Ni concentration.[26] According to Figs. 4(a) and 4(b), the corresponding values of $d\rho_{\rm res}/dx$ for Fe- and Ni-doped Y124 are $\approx 65.0$ mΩ cm per Fe concentration, and $\approx 90$ mΩ cm per Ni concentration. Using Eq. (1) we may find values of the *ab*-plane scattering rates for the single-crystal analog of the polycrystalline samples by using the formula

$$\frac{d\tilde{\rho}_{ab,\rm res}}{dx} = [\gamma(x)]^{-2/3}\frac{d\rho_{\rm res}}{dx} - \tfrac{2}{3}[\gamma(x)]^{-5/3}\rho_{\rm res}(x)\frac{d\gamma(x)}{dx} . \tag{2}$$

For low $x$ we evaluate the derivatives in Eq. (2) at $x = 0$ for which $\rho_{\rm res}(x) = 0$. So the second term on the right-hand side of Eq. (2) will be almost zero. Moreover, for Y123, $\gamma(0) = 8.8$ (Ref. 11). Thus $d\tilde{\rho}_{ab,\rm res} = 10.5$ mΩ cm (0.42 mΩ cm) per Fe (Ni) concentration in the Y123 system. According to Zech,[10] $\gamma_{124} \approx 2\gamma_{123}$. So for Y124 we take $\gamma(0) = 17.6$. This gives $d\tilde{\rho}_{ab,\rm res}/dx = 9.5$ mΩ cm (13.0 mΩ cm) per Fe (Ni) concentration in the Y124 system. If we calculate $d\tilde{\rho}_{ab,\rm res}/dx$ at $x = 0.01$, all the results will be reduced by about 15%. This is because according to Chien *et al.*[11] in the Fe-doped Y123 system and for $x < 0.013$ we may write $\gamma(x)$ as $\gamma(x) = \gamma(0) + Qx$ with $Q = d\gamma/dx = 150$. For Ni-doped Y123, and for Fe- and Ni-doped Y124, we also expect $Q$ to be near 150. Even if $Q$ is quite different for other than Fe-doped Y123 samples, the difference between the values of $d\tilde{\rho}_{ab,\rm res}/dx$ is so sharp (31 times for Ni-doped Y123 and Y124) that for the physically reasonable values of $Q$ this factor of 31 (for the Ni-doped system) cannot be reduced to, say, a factor of 2 or 3. In fact, the maximum effect of the value of $Q$ will be about 15% or a factor of about 1.2 only. The scattering rate per impurity $d(1/\tau)/dx$, where $\tau$ is the carrier relaxation time, is proportional to $n(d\tilde{\rho}_{ab,\rm res}/dx)$. Here $n$ is the planar carrier density.

On the basis of penetration-depth measurements in the Y123 and Y124 systems,[27] the planar carrier concentration in the Y124 system is smaller by a factor of 0.64 than that in the Y123 system. Combining this with the above-estimated values of $d\rho_{ab,\rm res}/dx$, we find that the carrier-impurity scattering rate in the Y124 systems is $6.0A$ for Fe and $8.3A$ for Ni, as against $10.5A$ for Fe and $0.42A$ for Ni in the Y123 system. Here $A$ is a parameter having dimensions of the scattering rate. The scattering rate of Fe-doped Y124 is less than that of the correspondingly (Fe-) doped Y123 system by a factor of about 1.7. Because of the uncertainty of about a factor of 1.8 (see the Appendix) due to the polycrystalline nature of the samples used, the ratio of the scattering rates per Fe concentration in the doped Y124 and Y123 systems will be reduced to about $1.7/1.8 = 0.94$. This means that the scattering rate per Fe concentration will remain less in the Y124 system than in the Y123 system. But if Fe has to suppress $T_c$ in Y124 relatively more strongly, the scattering rate per Fe concentration should be more in Y124 by about a factor of 7.0. This is because in Y124 (Y123) superconductivity is suppressed by Fe with $x \approx 2.2$ at. % ($x \approx 18.0$ at. %), and because $T_c$ of pure Y124 (Y123) is 78 K (90 K). In view of the conclusively large difference in the observed (0.94) and required (7.0) ratio of scattering rages per Fe concentration in Y124 and Y123, we conclude that in Fe-doped Y124 carrier-impurity scattering may not be a possible reason for $T_c$ degradation.

According to the above estimates, the scattering rate of Ni-doped Y124 will be about 20 times larger than that of the Ni-doped Y123 system. This is a very large factor,

and cannot be reduced below about $20/1.8 \approx 11.1$. On the other hand, for the interpretation of the observed[1,2] $T_c$ degradation in the Y123 and Y124 systems, the ratio of the scattering rates per Ni concentration in these systems should also be about 7.0. Thus in the case of the Ni-doped Y123 and Y124 systems the potential scattering does not seem to be a possible source of $T_c$ degradation. The situation will become clearer when single-crystal data become available.

### C. Direct suppression of pairing interaction

Since carrier-impurity potential scattering is found to be a doubtful source of $T_c$ degradation in Fe-doped Y124, and since localization is also doubtful, it is reasonable to consider as the source of suppression of superconductivity the direct suppression of the pairing interaction. Since the Fe and Ni dopants enter at the Cu sites, the pairing interaction will involve the Cu sites in an essential way. This means that from the viewpoint of the direct suppression of the pairing interaction only that type of pairing interaction will be reasonable in the superconducting phase of the considered system whose formation is significantly sensitive to the absence of the Cu atom at the impurity site. Spin fluctuations and excitons involve the Cu sites in an important manner so they are favorable for the pairing interaction from this point of view. On the other hand, plasmons, having their origin in a single (mainly O $2p$-based) band, are not obviously favorable.

In view of the above it is desirable to understand how the pairing interaction can be suppressed so drastically in the Fe- or Ni-doped Y124 system. Stacking faults in the Y124 system may be one of the reasons.[28] Local distortion around the impurity of the type observed[29] in Fe-, Co-, Ni-, or Zn-doped Y123 is another reasonable possibility.

## V. CONCLUSIONS

In conclusion, we have made measurements of the resistivity of polycrystalline samples of the Fe- and Ni-doped Y124 system. The behavior of the resistivity is much different from the Mott law of VRH for $T$ above about 30 K. While the Ni 5-at. % sample is expected to have NNH behavior in the resistivity above 150 K, no such indication is found in the Fe 10-at. % sample. Localization and the carrier-impurity scattering of magnetic or potential origin do not seem to be important for $T_c$ degradation in the Fe- and Ni-doped Y124 system. The direct suppression of the pairing interaction may be a reasonable source of $T_c$ degradation in the system studied.

## ACKNOWLEDGMENTS

Keen interest and continuous encouragement from Professor S. K. Joshi (Council of Scientific and Industrial Research) in the present work are gratefully acknowledged. Experimental help of B. V. Kumaraswamy for susceptibility measurements is also acknowledged.

## APPENDIX

In this Appendix we consider resistivity data of Zn- and Co-doped single crystals and polycrystalline samples of Y123, and examine how far the single-crystal analogs of the polycrystalline samples represent the real single crystals. The single-crystal analog of a polycrystalline sample is obtained by eliminating the $c$-direction resistivity by using Eq. (1). We shall consider the resistivity data of a single crystal of Zn-doped Y123 from Ref. 30, a single crystal of Co-doped Y123 from Ref. 31, a polycrystalline sample of Zn-doped Y123 from Ref. 32, and a polycrystalline sample of Co-doped Y123 from Ref. 33. We shall denote these four crystals, respectively, by *S*Zn, *S*Co, *P*Zn, and *P*Co. Let $d\rho_{ab,\mathrm{res}}/dx$ denote the rate of change of $ab$-plane residual resistivity of a single crystal with the impurity concentration. $d\tilde{\rho}_{ab,\mathrm{res}}/dx$ denotes (see text) the same quantity for the single-crystal analog of the polycrystalline sample. The value of $d\rho_{ab,\mathrm{res}}/dx$ and $d\rho_{\mathrm{res}}/dx$ are given in Table I. An interesting observation is that for Zn $d(\rho_{ab,\mathrm{res}},\rho_{\mathrm{res}})/dx$ varies rather sharply with $x$, while for Co this variation is much slower. This may be considered to imply that the effect of the impurity is qualitatively similar in both the single-crystal and polycrystalline samples.

In obtaining the values of $\rho_{ab,\mathrm{res}}$ or $\rho_{\mathrm{res}}$ for the *S*Co sample of $x=0.041$ and *P*Co sample of $x=0.0167$, we have considered the extrapolation of the values of these quantities from $T=250$ K to $T=300$ K. This is because, for these values of $x$, $\rho_{ab}$ for the single crystal (Ref. 31) and $\rho$ for the polycrystal (Ref. 33) decrease faster than a linear relation near $T_c$. For the *S*Co sample of $x=0.096$ and *P*Co sample of $x=0.010$, we have taken the values of $\rho_{ab,\mathrm{res}}$ and $\rho_{\mathrm{res}}$ on the basis of the values of $\rho_{ab}$ and $\rho$ near $T_c$. The reason for this is that for these samples of Co $\rho_{ab}$ or $\rho$ starts to become nearly independent of $T$ near $T=T_c$ (Refs. 31 and 33).

According to Table I the average values of $d\rho_{ab,\mathrm{res}}/dx$ for the *S*Zn and *S*Co samples are, respectively, 2.50 mΩ cm per Zn concentration and 2.62 mΩ cm per Co concentration. On the other hand, the average values of

TABLE I. $d\rho_{ab,\mathrm{res}}/dx$ for single crystals of Zn- and Co-doped Y123, and $d\rho_{\mathrm{res}}/dx$ from polycrystalline samples of Zn- and Co-doped Y123.

| Sample | $x$ | $d(\rho_{ab,\mathrm{res}},\rho_{\mathrm{res}})/dx$ (mΩ cm per impurity concentration) | Reference |
|---|---|---|---|
| Zn-doped | 0.0053 | 1.88 | 30 |
| single crystal | 0.036 | 3.11 | 30 |
| Co-doped | 0.041 | 2.43 | 31 |
| single crystal | 0.096 | 2.81 | 31 |
| Zn-doped | 0.02 | 10.52 | 32 |
| polycrystal | 0.053 | 8.80 | 32 |
| Co-doped | 0.0167 | 9.13 | 33 |
| polycrystal | 0.10 | 9.32 | 33 |

$d\rho_{res}/dx$ for the *P*Zn and *P*Co samples are 9.66 mΩ cm per Zn concentration and 9.23 mΩ cm per Co concentration, respectively. Taking $\gamma(0)=8.8$ (Ref. 11) and using Eq. (2) at the $x=0$ point, we obtain $d\tilde{\rho}_{ab,res}/dx=2.26$ mΩ cm per Zn concentration for *P*Zn and $d\tilde{\rho}_{ab,res}/dx=2.16$ mΩ cm per Co concentration for *P*Co. For Zn $d\tilde{\rho}_{ab,res}/dx$ is only about 10.0% different from $d\rho_{ab,res}/dx$, while for Co $d\tilde{\rho}_{ab,res}/dx$ is about 17.5% different from the corresponding value of $d\rho_{ab,res}/dx$. Noting that Zn goes mainly into the $CuO_2$ planes and Co goes mainly into the CuO chains, these changes provide an idea regarding the general nature of the single-crystal analogy of polycrystalline samples. Thus we may roughly take 17.5% as the upper limit of the difference in the values of $d\rho_{ab,res}/dx$ and $d\tilde{\rho}_{ab,res}/dx$. With Fe and Ni we do not expect much change in the upper limit, particularly because in Sec. IV B we have considered only low-$x$ samples of Fe and Ni. However, for safety we may assume that the maximum difference between $d\rho_{ab,res}/dx$ and $d\tilde{\rho}_{ab,res}/dx$ will not exceed, say, the limit of 25%. When this is so, the single-crystal analog of the polycrystalline sample will represent the resistivity of the polycrystalline sample in the *ab* plane to within a factor of about 1.33. This means that, in the case where we encounter a difference between $d\rho_{ab,res}/dx$ and $d\tilde{\rho}_{ab,res}/dx$ by a factor of much more than 1.33, the approximation of the single-crystal analog of polycrystalline samples will be a good approximation. In this sense, when we compare the resistivity of two polycrystalline samples, there will be an uncertainity of a factor of about $1.33\times1.33\approx1.8$. The above way of treating polycrystalline samples is expected to be useful for the Fe- and Ni-doped samples of Y124 also. This is because such samples are similar to the corresponding samples of Y123 in at least two ways. First, in both the Y123 and Y124 systems, Fe replaces mainly the Cu atoms on the chain sites, while Ni replaces mainly the Cu atoms on the planar sites.[34,35] Secondly, for low concentration ($x\leq0.03$) of Fe and Ni, the room-temperature resistivity, $\rho_{300}(x)$ rises by a similar factor. For example, for an Fe-doped sample of Y123 (Y124) the room-temperature resistivity assumes the values (in mΩ cm) 0.5 (0.8), 1.1 (1.75), 1.9 (2.4), and 2.7 (2.9) for $x=0$, 0.01, 0.02, and 0.03, respectively. In obtaining the values of the room-temperature resistivity for the Fe-doped Y123 system we have used interpolation of the values given in Ref. 36. On the basis of these values of $\rho_{300}(x)$ we see that $\rho_{300}(0.01)/\rho_{300}(0)$ is almost the same, 2.2, in the cases of the Y123 and Y124 systems. For $x=0.02$ and 0.03, $\rho_{300}(x)/\rho_{300}(0)$ is less for the Y124 system, implying that the contribution of the *c*-axis resistivity will be less in the Fe-doped Y124 system than in the Y123 system. Thus for $x\leq0.03$ we may use similar anisotropy variation with Fe and Zn doping in the Y123 and Y124 systems.


[1]A. V. Narlikar, C. V. Narsimha Rao, and S. K. Agarwal, in *Studies of High Temperature Superconductors,* edited by A. V. Narlikar (Nova Science, New York, 1990), Vol. 1, p. 370.

[2]R. Lal, S. P. Pandey, A. V. Narlikar, and E. Gmelin, Phys. Rev. B **49**, 6382 (1994).

[3]G. Deutscher, A. Palevski, and R. Rosenbaum, in *Localization, Interaction, and Transport Phenomenon* edited by B. Kramer, G. Bergmann, and Y. Bruynsesaede (Springer-Verlag, Berlin, 1985), pp. 108–120.

[4]A. A. Abrikosov and L. P. Gorkov, Sov. Phys. JETP **12**, 1243 (1961).

[5]A. J. Mills, S. Sachdev, and C. M. Varma, Phys. Rev. B **37**, 4975 (1988).

[6]This is possible when the impurity interacts strongly with those bosons which are responsible for mediating pairing interaction between the carriers of the system, or when there is a change in the carrier concentration.

[7]R. E. Walstedt *et al.*, Phys. Rev. B **48**, 10 646 (1993).

[8]For *s*-wave pairing, see P. Chaudhari and Shawn-Yu Lui, Phys. Rev. Lett. **72**, 1084 (1994); A. G. Sun, D. A. Gajewski, M. B. Maple, and R. C. Dynes, *ibid.* **72**, 2267 (1994); G. D. Mahan, *ibid.* **71**, 4277 (1993).

[9]For *d*-wave pairing, see B. G. Levi, Phys. Today **46**, (5), 17 (1993).

[10]C. D. Zech, Phys. Rev. B **48**, 6533 (1993).

[11]T. R. Chien, W. R. Datars, M. D. Lan, J. Z. Liu, and R. N. Shelton, Phys. Rev. B **49**, 1342 (1994).

[12]R. N. Bhatt, P. Wolfle, and T. V. Ramakrishnan, Phys. Rev. B **32**, 569 (1985).

[13]In fact, $\rho(x)=[\rho_a(x)\rho_b(x)\rho_c(x)]^{1/3}$. Now since $\gamma(x)=[\rho_c(x)/\rho_{ab}(x)]^{1/2}$ and $\rho_{ab}(x)=[\rho_a(x)\rho_b(x)]^{1/2}$ we obtain $\tilde{\rho}_{ab}(x)=[\gamma(x)]^{-2/3}\rho(x)$.

[14]B. P. Singh, S. P. Pandey, B. V. Kumaraswamy, and A. V. Narlikar, Phys. Rev. B **46**, 3573 (1992).

[15]K. Yanagisawa, Y. Matsui, Y. Kodama, Y. Yamada, and T. Matsumoto, Physics C **191**, 32 (1992).

[16]S. Pradhan, D. McDaniel, A. Killing, W. Huff, P. Boolchand, and D. E. Farrel, Bull. Am. Phys. Soc. **35**, 208 (1990).

[17]Y. Kodama, Y. Yamada, N. Murayama, N. Avano, and I. Matsumoto, in *Advances in Superconductivity III,* edited by K. Kajimura and H. Hayakawa (Springer-Verlag, Tokyo, 1991), p. 339.

[18]T. Miyatake, S. Gotoh, N. Koshizuka, and S. Tanaka, Nature **341**, 41 (1989).

[19]S. Tanda, K. Takahashi, and T. Nakayama, Phys. Rev. B **49**, 9260 (1994).

[20]This conclusion is based on Fig. 1 and Table I of Ref. 19.

[21]N. F. Mott, Philos. Mag. **19**, 835 (1969).

[22]B. Abeles, P. Sheng, M. D. Goutts, and Y. Arie, Adv. Phys. **24**, 407 (1975); A. L. Efros and B. I. Shklovskii, J. Phys. C **8**, L49 (1975).

[23]B. I. Shklovskii and A. L. Afros, *Electronic Properties of Doped Semiconductors* (Springer-Verlag, Berlin, 1984), Chap. 9.

[24]The value of *g* is taken from J. Yu, K. T. Park, and A. J. Freeman, Physica C **172**, 4679 (1991).

[25]J. M. Tarascon, P. Barboux, P. F. Micel, L. H. Greene, G. W. Hull, M. Eibschutz, and S. A. Sunshine, Phys. Rev. B **37**, 7458 (1988).

[26]J. M. Tarascon, W. R. McKinnon, L. H. Greene, G. W. Hull, and E. M. Vogel, Phys. Rev. B **36**, 8393 (1987).

[27]H. Keller *et al.*, Physica C **185-189**, 1089 (1991).

[28]J. C. Phillips (private communication).
[29]F. Bridges, G. Li, J. B. Broyce, and T. Claeson, Phys. Rev. B **48**, 1266 (1993); G. Li, F. Bridges, J. B. Boyce, and W. Ch. Jainer, Phys. Rev. B **47**, 12 210 (1993).
[30]T. R. Chien, Z. Z. Wang, and N. P. Ong, Phys. Rev. Lett. **67**, 2088 (1991).
[31]A. Carrington, A. P. Mackenzie, C. T. Lin, and J. R. Cooper, Phys. Rev. Lett. **69**, 2855 (1992).
[32]G. Ilonca, M. Mehbod, A. Lanckbeen, and R. Deltour, Phys. Rev. B **47**, 15 265 (1993).
[33]B. Fisher, J. Genossar, L. Patlagan, and G. M. Reisner, Phys. Rev. B **48**, 16 056 (1993).
[34]A. V. Narlikar, S. K. Agarwal, and C. V. N. Rao, in *Studies of High Temperature Superconductors* (Ref. 1), p. 341.
[35]That Fe (Ni) substitutes for Cu in the chain (plane) of Y124 is shown by high-resolution transmission electron microscope studies. See Y. Matsui and K. Yanagisawa, in *Studies of High Temperature Superconductors,* edited by A. Narlikar (Nova Science, New York, 1993), Vol. 11, p. 437.
[36]G. Kallias, I. Panagiotopoulos, D. Niarchos, and A. Kostikas, Phys. Rev. B **48**, 15 992 (1993).